SUPPLEMENTAL

Structure-based design of a small molecule CD4-antagonist with broad spectrum anti-HIV-1 activity

Francesca Curreli[a¶], Young Do Kwon[b¶], Hongtao Zhang[a], Daniel Scacalossi[a], Dmitry S. Belov[c], Artur A. Tikhonov[c], Ivan A. Andreev[c], Andrea Altieri[c], Alexander V. Kurkin[c], Peter D. Kwong[b] & Asim K. Debnath[a*]

[a]Laboratory of Molecular Modeling and Drug Design, Lindsey F. Kimball Research Institute, New York Blood Center, New York, NY 10065, USA.

[b]Vaccine Research Center, National Institute of Allergy and Infectious Diseases, National Institutes of Health, Bethesda, MD 20892, USA.

[c]EDASA Scientific, Scientific Park, Moscow State University, Leninskie Gory, Bld.75, 77 – 101b; 119992 Moscow - Russia

¶ These authors contributed equally.

Address for communication: Dr. Asim K Debnath (adebnath@nybloodcenter.org)

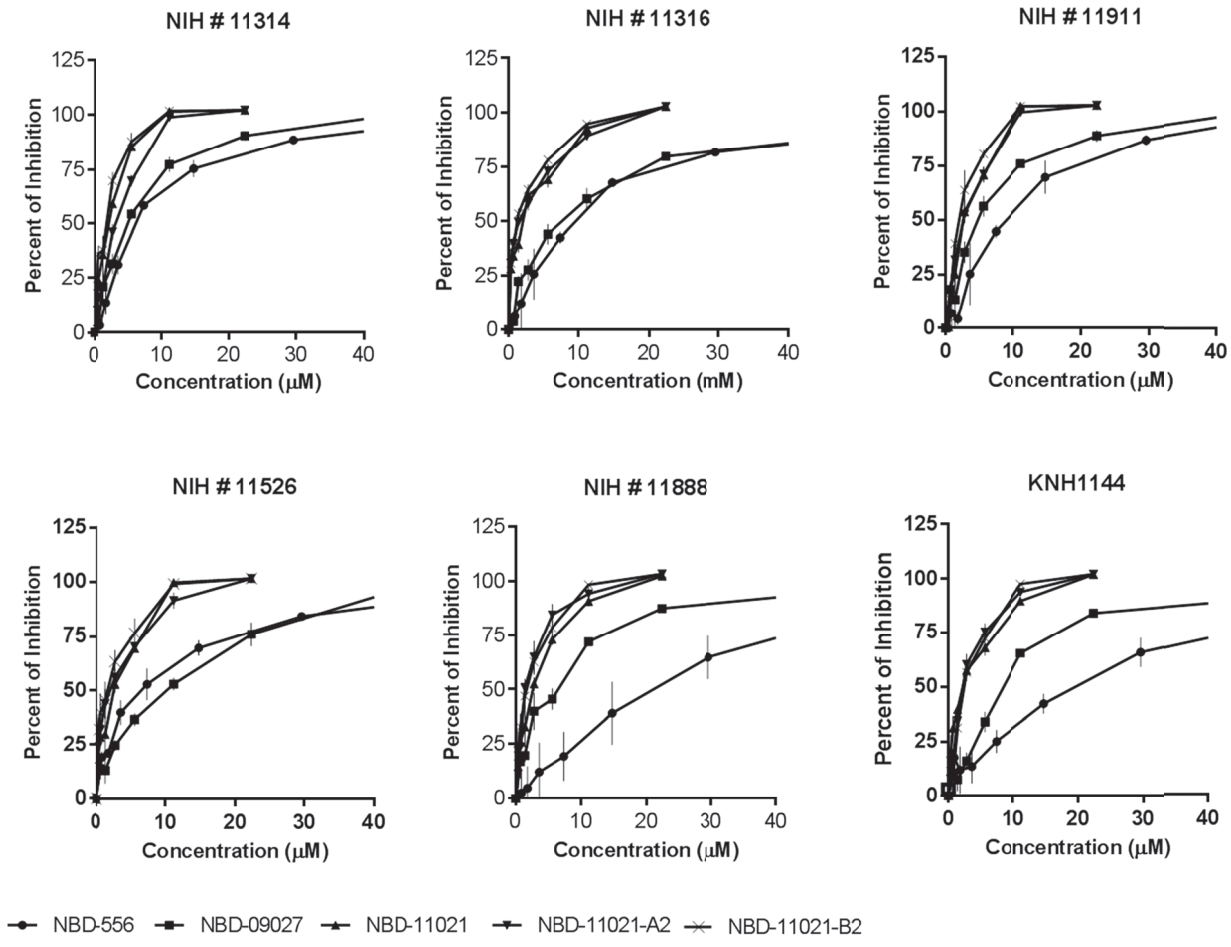

Figure S1: Representative dose-dependent inhibition of NBD compounds against ENV-pseudotyped HIV–1. Experiments were performed in triplicate, and data is shown as mean ± standard deviation.

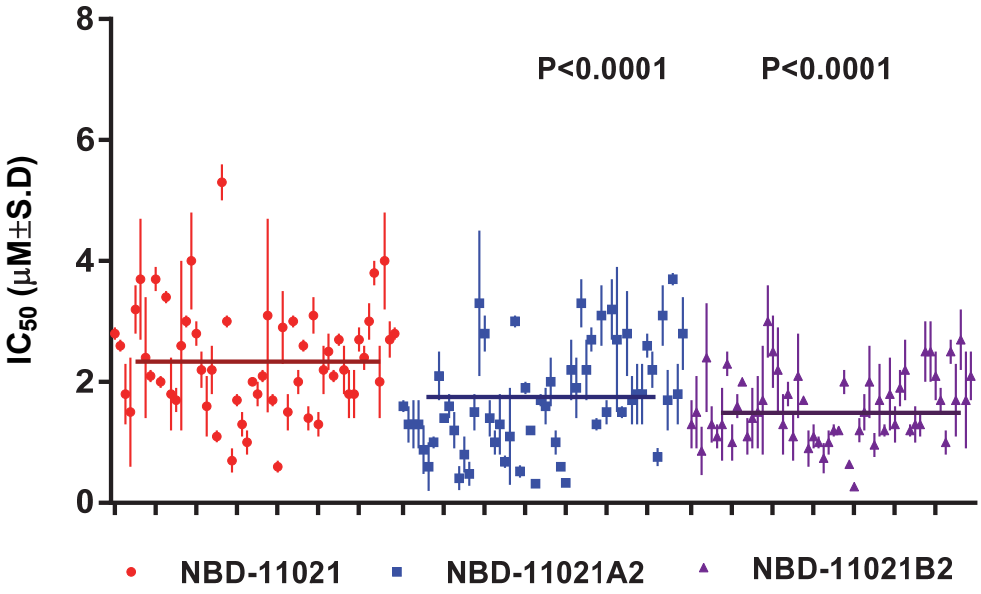

	NBD-11021	NBD-11021A2	NBD-11021B2
Mean ± Std Error of Mean	2.38 ± 0.12	1.71 ± 0.12	1.57 ± 0.08

Figure S2. Comparison of IC_{50} of fractions NBD-11021-A2 and NBD-11021-B2 versus NBD-11021 tested on a large panel of HIV-1 ENV-pseudoviruses including primary and transmitted/founder HIV-1 isolates from different clades. Statistical testing was conducted with the one-way ANOVA, implementing Dunnett's test for adjustments of multiple comparisons, with a significance level set at 0.05.

NBD-11021A1 &NBD-11021A2 in $CDCl_3$

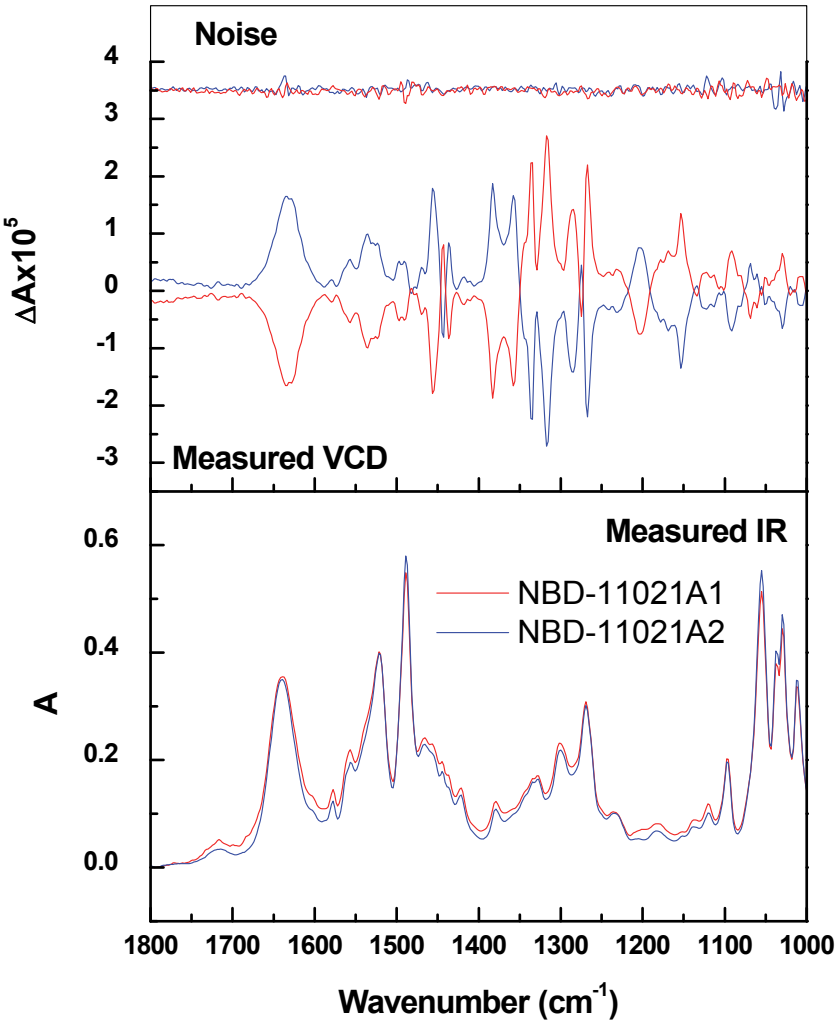

Figure S3: IR (lower frame) and VCD (upper frame) spectra of **NBD-11021A1 and NBD-11021A2** in $CDCl_3$ (10mg/0.2mL); 0.1mm path-length cell with BaF_2 windows; 6 h collection for samples and solvent; instrument optimized at 1400 cm^{-1}. Solvent-subtracted IR and enantimer-subtracted VCD spectra are shown. Uppermost trace is the VCD noise spectra.

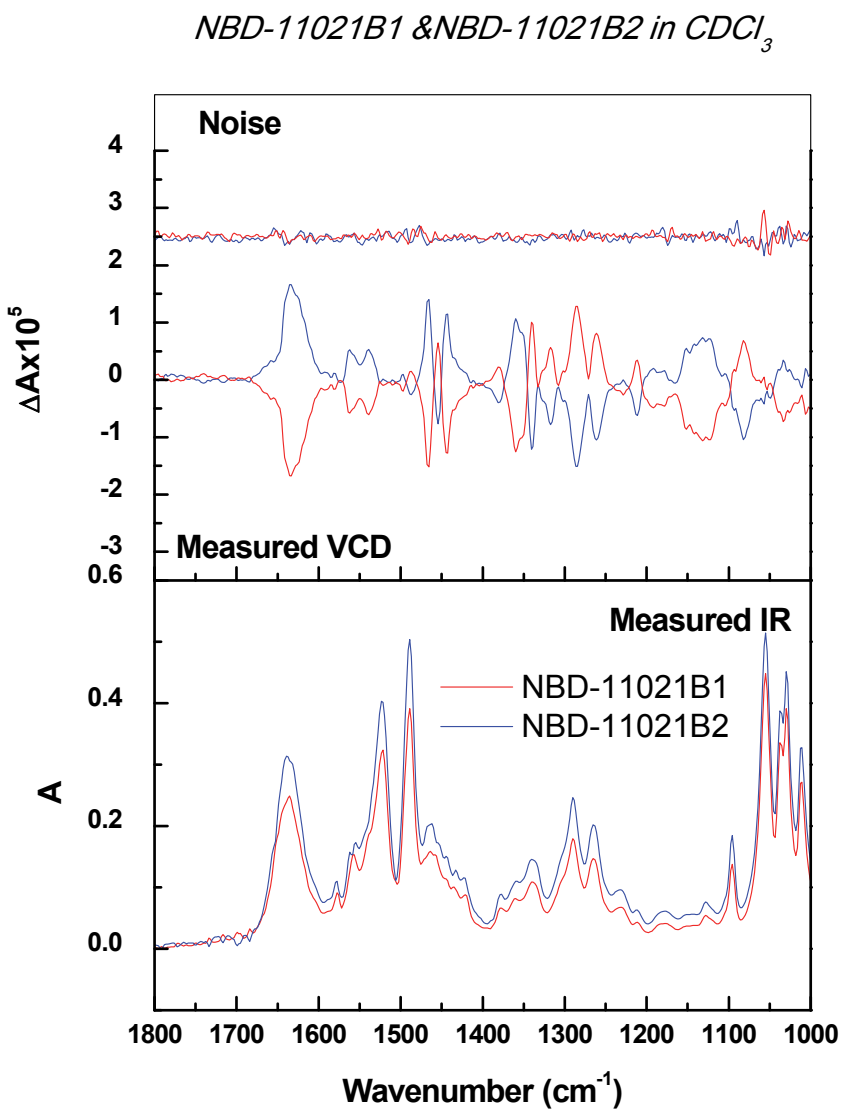

Figure S4: IR (lower frame) and VCD (upper frame) spectra of **NBD-11021B1 and NBD-11021B2** in $CDCl_3$ (10mg/0.2mL); 0.1mm path-length cell with BaF_2 windows; 6 h collection for samples and solvent; instrument optimized at 1400 cm^{-1}. Solvent-subtracted IR and enantimer-subtracted VCD spectra are shown. Uppermost trace is the VCD noise spectra.

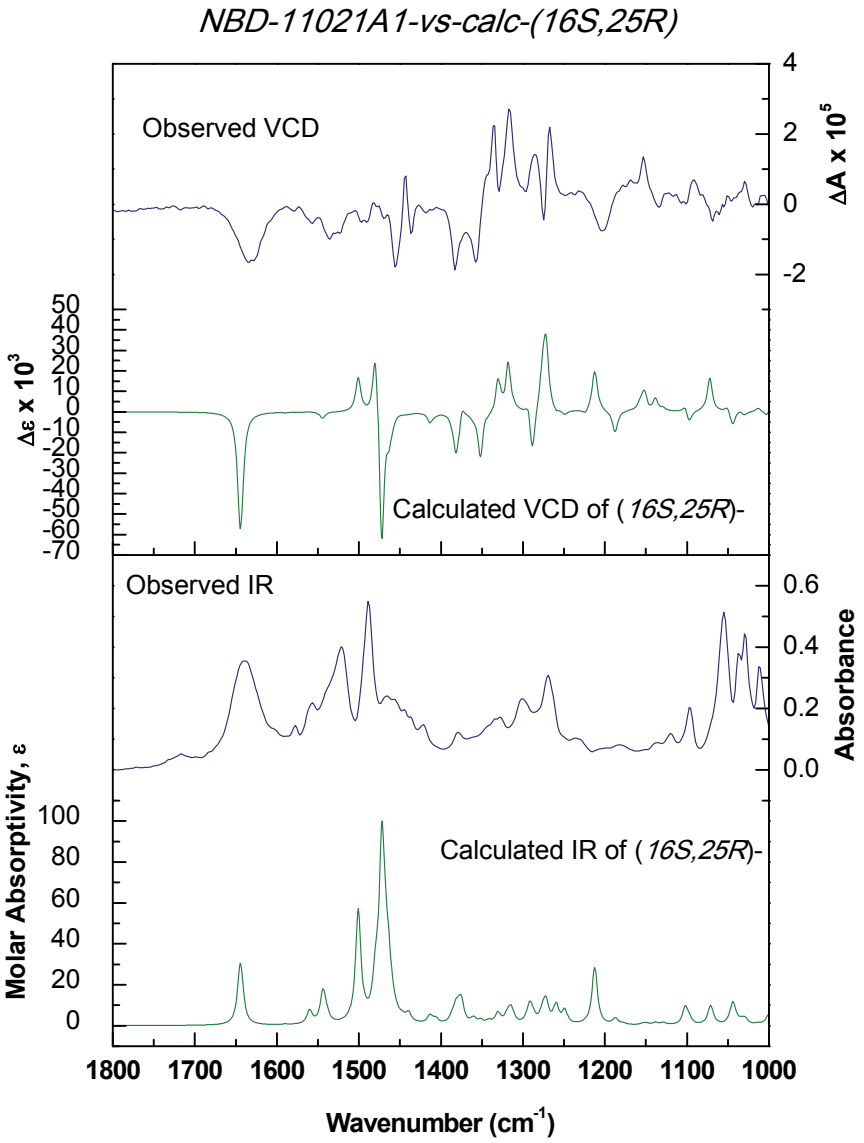

Figure S5: IR (lower frame) and VCD (upper frame) spectra observed for **NBD-11021A1** (right axes) compared with calculated Boltzmann-averaged spectra of the calculated conformations for the (*16S,25R*)- configuration (left axes).

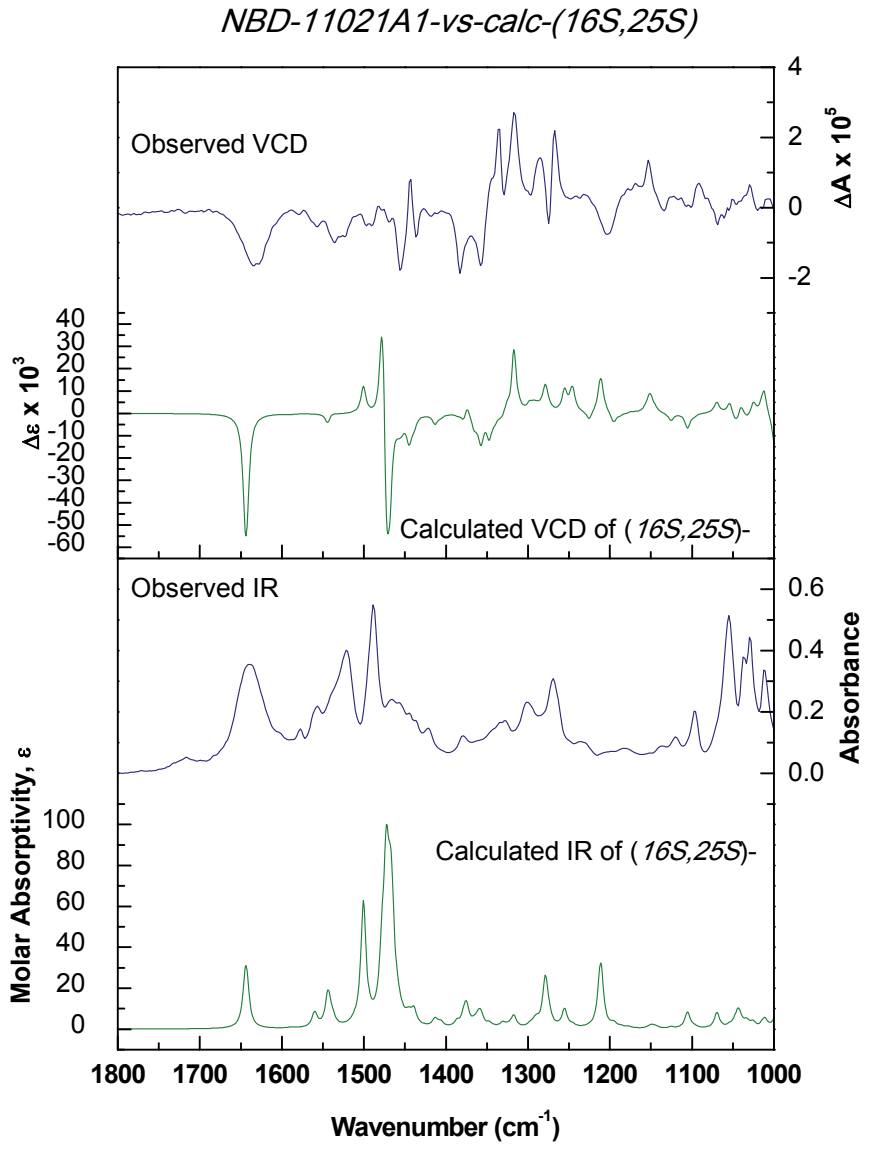

Figure S6: IR (lower frame) and VCD (upper frame) spectra observed for **NBD-11021A1** (right axes) compared with calculated Boltzmann-averaged spectra of the calculated conformations for the (*16S,25S*)- configuration, (left axes).

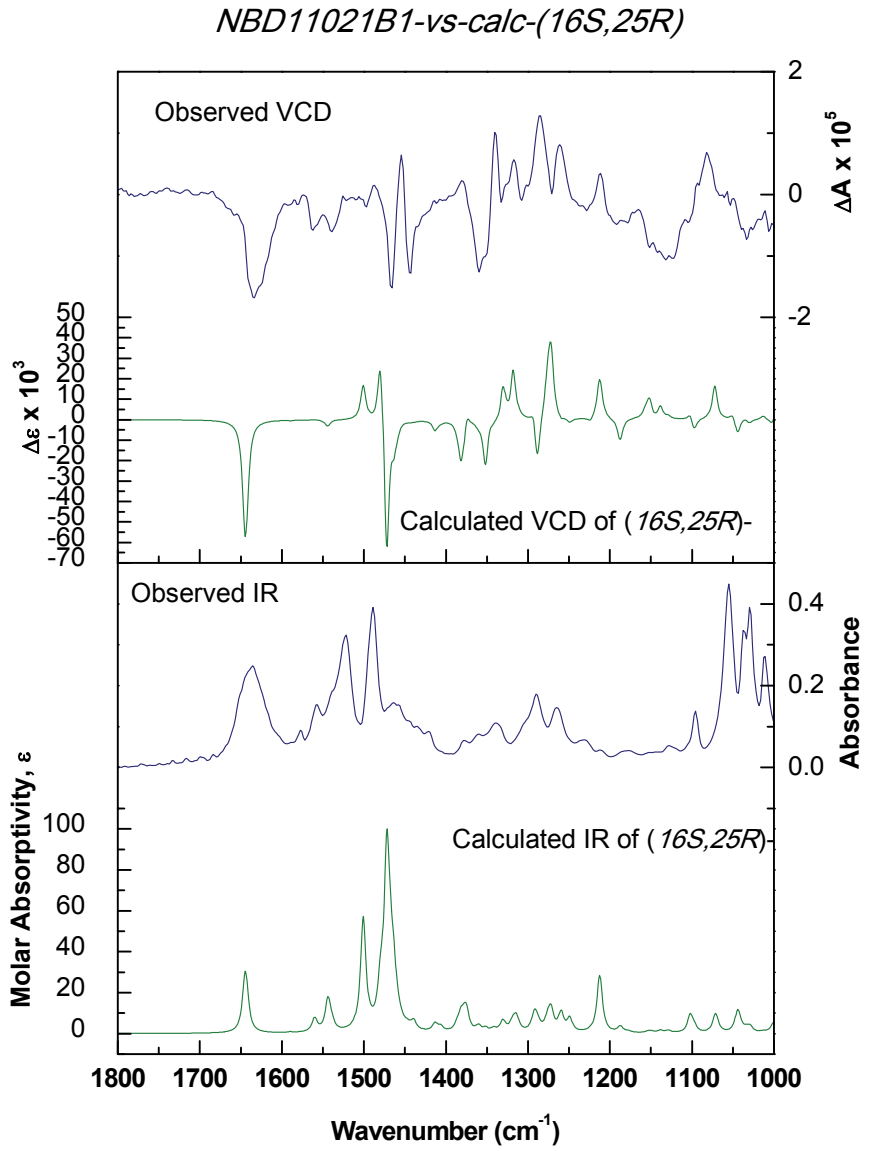

Figure S7: IR (lower frame) and VCD (upper frame) spectra observed for **NBD-11021B1** (right axes) compared with calculated Boltzmann-averaged spectra of the calculated conformations for the (*16S,25R*)- configuration, (left axes).

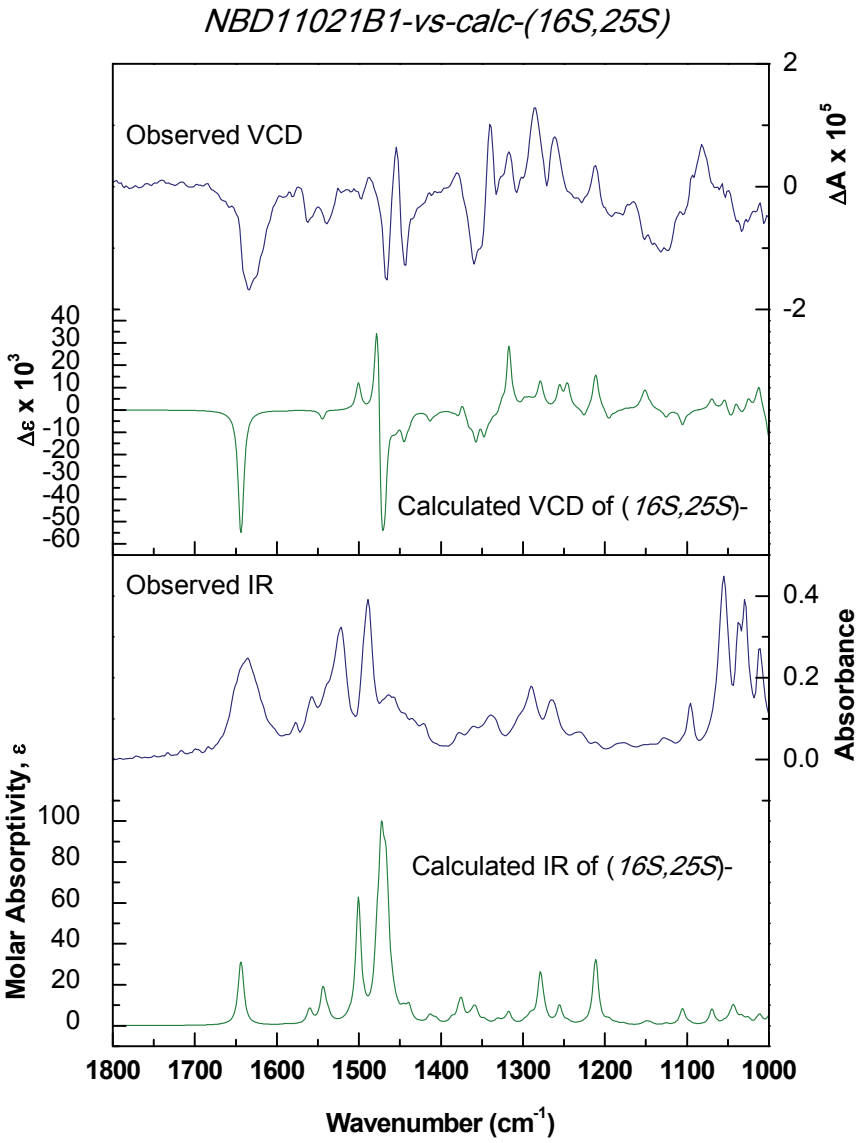

Figure S8: IR (lower frame) and VCD (upper frame) spectra observed for **NBD-11021B1** (right axes) compared with calculated Boltzmann-averaged spectra of the calculated conformations for the (*16S,25S*)- configuration, (left axes).

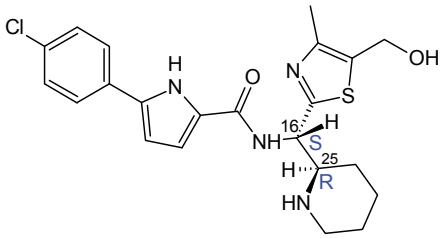

Structure of NBD-11021A1

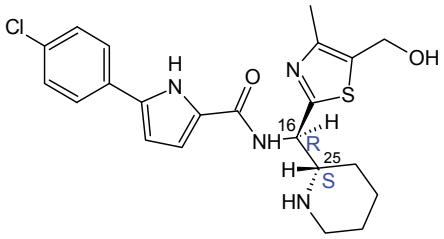

Structure of NBD-11021A2

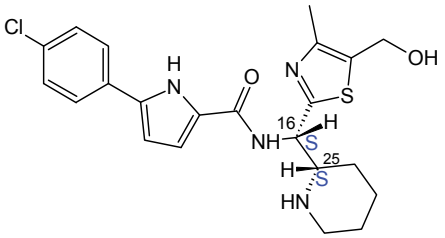

Structure of NBD-11021B1

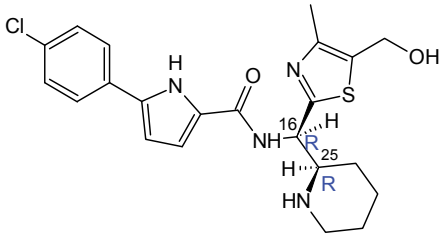

Structure of NBD-11021B2

Figure S9: Assignment of the absolute configuration of NBD-11021A1, NBD-11021A2, NBD-11021B1 and NBD-11021B2.

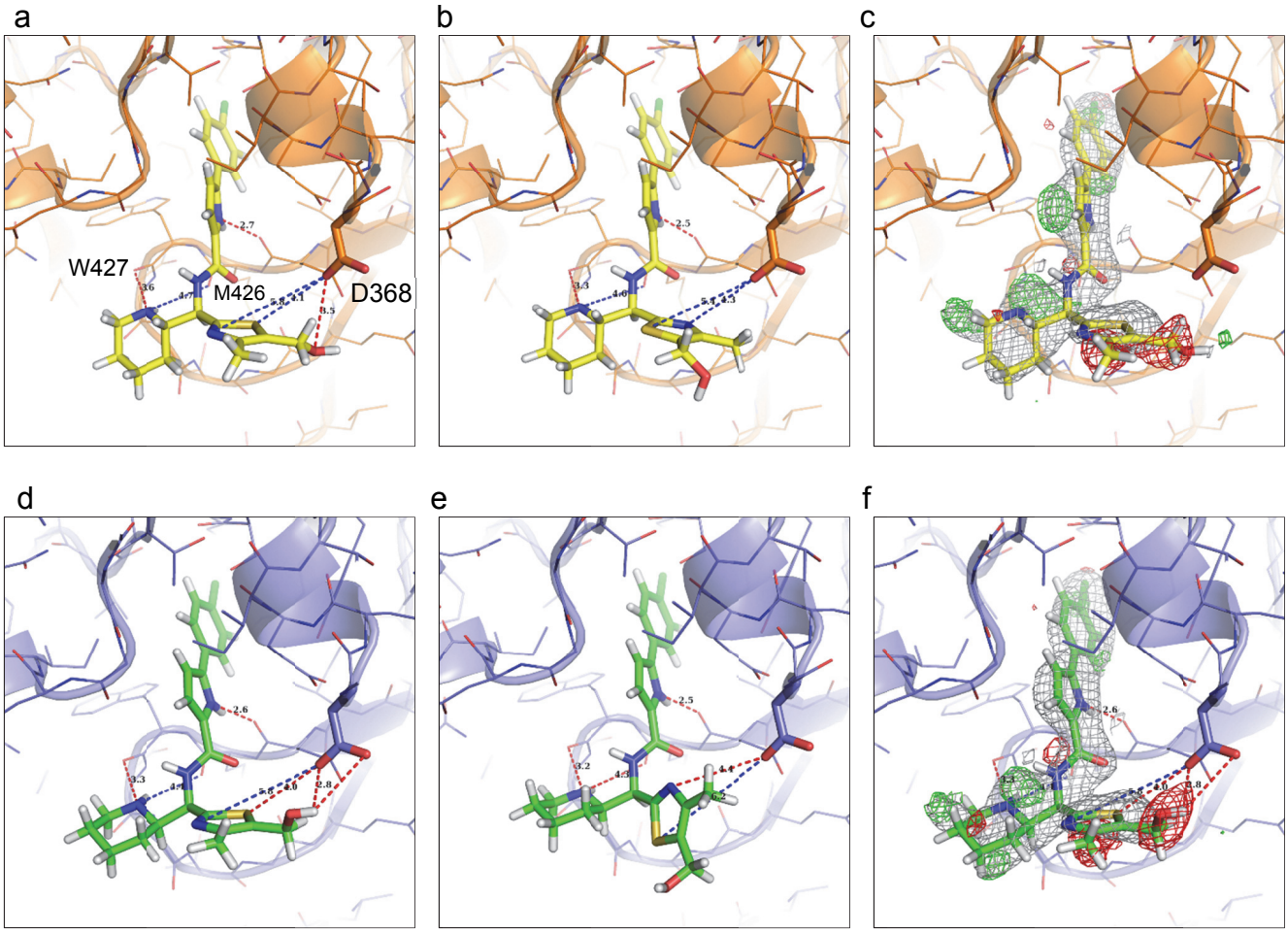

Figure S10. Putative binding modes of NBD-11021A2 (R,S) and NBD-11021B2 (R,R) enantiomers into the Phe 43 cavity. (a, b) The thiazole rings of NBD-11021A2 enantiomer face Asp368, which enables either the nitrogen atom or the sulfur atom to make H-bond contacts with Asp368. (c) When the NBD-11021A2 enantiomer modeled in (a) was refined, strong negative *fofc* electron density (red mesh, contoured at -3σ) appeared at the methyl group and hydroxymethyl group of thiazole ring, indicating that the thiazole ring is not a good fit. Gray mesh, *2fofc* electron density contoured at 1σ, green mesh, positive *fofc* electron density map contoured at 3σ. (d, e) The thiazole rings of NBD-11021B2 enantiomer face Asp368, which enables either the nitrogen atom or the sulfur atom to make H-bond contacts with Asp368. (f) When the NBD-11021B2 enantiomer modeled in (d) was refined, strong negative *fofc* electron density (red mesh, contoured at - 3σ) appeared at the methyl group and hydroxymethyl group of thiazole ring, indicating that the thiazole ring is not a good fit. Gray mesh, *2fofc* electron density contoured at 1σ, green mesh, positive *fofc* electron density map contoured at 3σ.

Table S1. Crystallographic data collection and refinement statistics

	NBD-11021: 93TH057(H375S)
PDB accession code	4RZ8
Data collection	
Space group	$P2_1$
Cell constants	
a, b, c (Å)	113.6, 68.8, 116.1
α, β, γ (°)	90.0, 110.6, 90.0
Wavelength (Å)	1.00
Resolution (Å)	50.0-1.82(1.86-1.82)*
R_{merge}	6.7 (48.7)
$I / \sigma I$	19.9 (1.3)
Completeness (%)	87.5 (28.1)
Redundancy	3.4 (1.8)
Refinement	
Resolution (Å)	44.0-1.9
Unique reflections	124,367
R_{work} / R_{free} (%)	22.6/24.3
No. atoms	
Protein	10,579
Ligand/ion	740
Water	692
B-factors (Å^2)	
Protein	57.9
Ligand/ion	68.0
Water	52.9
R.m.s. deviations	
Bond lengths (Å)	0.001
Bond angles (°)	0.422
Ramachandran	
Favored regions (%)	96.5
Allowed regions (%)	3.5
Disallowed regions (%)	0.0

*Values in parentheses are for highest-resolution shell

Table S2. Neutralization activity of NBD-compounds against SIV, SHIV and a set of HIV-2 isolates

	IC_{50} (μM±SD)[a]		
Virus	**NBD-556**	**NBD-09027**	**NBD-11021**
SIV_{mac186}	12±0.9	6.2±0.4	≥11
$SHIV_{SF162P3}$	14.2±2.1	-	8.9±0.4
HIV-2_{CBL-23}	29±1	-	17.3±0.5
HIV-2_{CBL-20}	34.3±0.6	-	14.8±0.4
HIV-$2_{CDC310319}$	36.1±3.5	-	14.1±1
HIV-$2_{CDC310072}$	≥27	≥13	≥14
HIV-$2_{MVP-11971}$	10.4±1.3	6.6±0.8	≥16
HIV-2_{D194}	16.8±3.4	9.4±1.3	≥16

[a]Values representing the mean ± standard deviation (SD) were obtained from three independent experiments.